J Mater Sci: Mater Med (2008) 19:2157–2163
DOI 10.1007/s10856-007-3307-z

In vitro evaluation of poly(caporlactone) grafted dextran (PGD) nanoparticles with cancer cell

P. Prabu · Atul A. Chaudhari · Santosh Aryal · N. Dharmaraj · S. Y. Park · W. D. Kim · H. Y. Kim

Received: 26 May 2007 / Accepted: 8 October 2007 / Published online: 28 November 2007

Abstract This study dealt with the preparation and characterization of coumarin-6 loaded poly(caprolactone) grafted dextran (PGD) nanoparticles (NPs) and evaluation of cellular uptake by using human gastric cancer cell line (SNU-638), in vitro. The potential application of these PGD NPs for sustained drug delivery was evaluated by the quantification and localization of the cellular uptake of fluorescent PGD NPs. Coumarin-6 loaded PGD NPs were prepared by a modified oil/water emulsion technique and characterized by various physico-chemical methods such as, laser light scattering for particle size and size distribution, atomic force microscopy (AFM), zeta-potential and spectrofluorometry to identify the release of fluorescent molecules from the NPs. SNU-638 was used to measure the cellular uptake of fluorescent PGD NPs. Confocal laser scanning microscopic images clearly showed the internalization of NPs by the SNU-638 cells. Cell viability was assessed by treating the SNU-638 cells with PGD NPs for 48 h. The results reveal, that these biodegradable polymeric NPs holds promise in biomedical field as a carrier.

P. Prabu
Department of Bionanosystem Engineering, Chonbuk National University, Jeonju 561-756, Republic of Korea

A. A. Chaudhari · S. Y. Park
College of Veterinary Medicine, Chonbuk National University, Jeonju 561-756, Republic of Korea

S. Aryal
Center for Healthcare Technology Development, Chonbuk National University, Jeonju 561-756, Republic of Korea

N. Dharmaraj
Department of Chemistry, Bharathiar University, Coimbatore 641 046, India

W. D. Kim
Department of Future Technology, Korea Institute of Machinery and Materials, 171 Jang-dong, Yuseong-gu, Daejeon 305-343, Republic of Korea

H. Y. Kim (✉)
Department of Textile Engineering, Chonbuk National University, Jeonju 561-756, Republic of Korea
e-mail: khy@chonbuk.ac.kr

1 Introduction

Since decades, there has been a growing interest in developing biodegradable polymeric nanoparticles (NPs) as effective drug delivery devices. Various polymers have been used in drug delivery research as they can effectively deliver the drug to a target site and thus increase the therapeutic benefit, while minimizing the side effects [1]. Particle size and surface characteristics are the two major determinants of the NPs for clearance kinetics and biodistribution of colloidal particles in the body [2]. The size of a particle should be small enough (less than 200 nm) to avoid any mechanical clearance by filtration (phagocytes) [3]. Therefore, there is an urgent need to develop the system that diminishes the identification by reticuloendothelial system. For this purpose, biologically occurring molecules such as peptides, carbohydrates, lipids could hold promise [4].

Novel biodegradable polymers with desired hydrophobic/hydrophilic balance and degradation rate are important for application in sustained drug release. The synthetic polymer poly(caprolactone) (PCL) is attractive due to several reasons, such as, low cost, biocompatibility, sustained degradability, availability at low molecular weight, and excellent drug permeability [5, 6]. Moreover, PCL is a FDA-approved biodegradable polymer that has been used

in drug delivery [7–9]. On the other hand, dextran is a polysaccharide consisting of glucose molecules (biologically occurring molecules) coupled into long branched chains, mainly through a 1, 6- and some through a 1,3-glucosidic linkage. Dextrans are colloidal, hydrophilic and water-soluble substances, inert in biological systems and do not affect cell viability. Owing to these beneficial properties, dextrans have been used for many years as blood expanders to maintain or replace blood volume, and studied as a carrier system for a variety of therapeutic agents including antidiabetics, antibiotics, anticancer drugs, peptides and enzymes [10, 11]. Dextrans can also be easily degraded by the enzyme dextranase, present in the colon [12], and moreover the presence of dextran was shown to reduce or to avoid complement activation to decrease interactions with macrophage-like cell lines [13, 14], and to increase the circulation time of the nanoparticles [15]. The same polysaccharides have been used to modify the surface characteristics of biodegradable nanoparticles [16]. Taking advantage of these properties, dextran based polymeric prodrugs for colonic drug delivery was previously reported [17].

Much of the pervious reports mainly focused on the preparation and characterization of block copolymeric micelles as drug carriers using diblock and triblock copolymer. In the present work, based on the above facts and significance of PCL and dextran as good candidates for biomedical application, we undertake the formulation copolymer micelle system from PGD graft copolymers as a potential drug delivery vehicle. The polymer required for the nanoparticle formulation was prepared by the ring opening polymerization as reported previously [18, 19]. The formulation of micellic NPs was prepared by a modified oil/water emulsion technique in the presence of PVA as a stabilizer which were then characterized by various state-of-the-art techniques such as laser light scattering (DLS), atomic force microscopy (AFM) and zeta-potential. The in vitro fluorescence release from the nanoparticles was measured by fluorescence microplate reader. Cellular uptake of the coumarin-6 loaded nanoparticles and intracellular location of the nanoparticles were investigated by confocal laser scanning microscopy (CLSM), using human gastric cancer cell line (SNU-638).

2 Materials and methods

2.1 Materials

Dextran (average molecular weight 10,400), HMDS (1,1,1,3,3,3-hexamethyldisilazan) were purchased from Sigma Co., USA. CL(caprolactone), stannous octoate ($Sn(oct)_2$), poly(vinyl) alcohol (PVA) (molecular weight 65000) where purchased from Aldrich for polymerization, Fourier transmission infra red (FTIR) spectrum of the sample was recorded (as KBr) pellet using Bio-Rad Win spectrophotometer. Dicholormethane (DCM) and coumarin-6 were purchased from Aldrich Co., USA.

2.2 Methods

2.2.1 Formulation of PGD NPs

Four different samples of Poly(caprolactone) grafted silylated dextran (PGSD) copolymers were synthesized according to a previously reported method [18, 19], with different feeding ratios (Table 1) and were hydrolyzed by 1 M HCl to get PGD copolymer. PGD NPs were prepared by a modified oil/water emulsion method [20]. In brief 1 mg of polymer was dissolved in DCM (10 mL) and added drop wise into 0.1% PVA aqueous at the rate of 1 ml/min under sonication at room temperature. The organic phase was allowed to evaporate under reduced pressure until the final volume of the aqueous suspension was reduced to 20 mL. Finally the suspension was filtered by a micro filter with 0.22 μm pore size to remove polymer aggregates and 0.3 mg of such aggregate was obtained after filtration. Similarly coumarin-6 (0.05 % (w/v)) loaded fluorescent NPs also prepared by making polymer/coumarin-6 blend solution in DCM.

2.2.2 Characterization of NPs

Particle size and size distribution: Average particles size and size distribution were determined by DLS (Malvern System 4700 instrument Co., USA) equipped with vertically polarized light supplied by an argon-ion laser (Cyonics) operated at 20 mW. All experiments were performed at room temperature (25 °C) at a measuring angle of 90° to the incident beam.

Surface charge: Zeta-potential of the nanoparticles was determined by ELS measurement (ELS 8000/6000 Otsuka electronics Co., Japan) at 25 °C at a measuring angle of 20° to the incident beam. Before each analysis, samples were sonicated in an ultra-sonicator bath for a minute. All the measurements were repeated three times and the values reported are the mean ± S.D.

Surface morphology: Surface morphology of polymeric nanoparticles was observed by AFM Nanoscope IV multimode (Digital Instrument, Co. USA) in tapping mode using a Si cantilever with a spring constant of 3.5 N/m and a resonance frequency of 75 kHz. Scanning was performed at a scan speed of 1.85 Hz with a resolution of

512 × 512 pixels. Samples for AFM observation were prepared by placing a drop (10 μL) on the argon dried Si (1 1 1) wafers and allowed to form a film.

In-vitro release of fluorescent markers from nanoparticles: Coumarin-6 loaded nanoparticles were dispersed in transport buffer (stimulated body fluid) at pH 7.4, which used as simulate physiological fluid. The buffer solution was kept in an orbital shaker at constant gentle shaking of 110 rpm at 37 °C. At regular time intervals, the suspensions were centrifuged at 11,000*g* for 8 min. The precipitated particles were re-suspended in fresh buffer and placed back into the shaker. The supernatant containing released fluorescent marker was then analyzed by microplate reader to determine the percentage release of the fluorescent markers from the NPs.

2.3 Cell line experiment

2.3.1 Cell culture

Human gastric cancer cell line (SNU-638) was obtained from Korean cell line bank (Korea) and maintained in a RPMI 1640 (Gibco BRL Co., USA) culture medium supplemented with 10% (v/v) fetal bovine serum (Gibco BRL Co., USA) and antibiotics (100 μg/mL gentamycin and 100 μg/mL penicillin-streptomycin).

2.3.2 In-vitro cellular uptake of NPs

For quantitative study, SNU-638 cells were seeded into 6-well plates. After the cells reached 80% confluence, the medium was changed with those containing coumarin-6-loaded NPs. The cells with NPs were incubated for 2 h. After incubation, the media was removed and the cells were washed three times with PBS to eliminate the traces of NPs left in the wells. After that 0.5% Triton X-100 in 0.2 N NaOH was added to lyse the cells. The cells were collected and the amount of fluorescence was measured by fluorescence plate reader (SpectraMax fluorometer with SoftMax Programme, Molecular Probes Co., USA) with excitation wavelength at 430 nm and emission wavelength at 485 nm [21].

For qualitative study, cells were seeded in the 1 mL petri dish. Cells were washed for four times after 2 h incubation and then fixed with 75% ethanol for 15 min. The cells were further washed twice with PBS and the nuclei were counterstained with propidium iodide (PI) for 30 min. The cell monolayer was washed twice with PBS and observed by confocal laser scanning microscope (CLSM) (Zeiss LSM 410, USA) with imaging software (Fluoview FV300).

2.3.3 In-vitro cell viability test

The SNU-638 cells were plated at 1.0×10^4 cells in a 6-well plate, and incubated at 37 °C for 48 h. The cells were pretreated with 50 μL of NPs doses (PGD-3, 5, 10, and 20). The cell morphology was photographed using a camera attached to an optical microscope, and the cell viability was determined using the crystal violet staining method, as reported elsewhere [22].

3 Result and discussion

3.1 Characterization

The chemistry of PGD formation can be well explained by the different vibrational modes of both polyester and polysaccharides (Fig. 1). One can find the spectral insight in the range 1,000–1,750 cm^{-1}, sharp carboxyl stretching at 1,750 cm^{-1}along with glycisidic C–H around 2,900 cm^{-1} corresponding to the PGD copolymer [14]. No doubt, one should expect polyester C–H stretching in the same area i.e., 2,900 cm^{-1}, however, broadness of the band provided an evidence for its contribution due to dextran. These IR spectral features demonstrated the formation of expected PGD block copolymer. The spectral analysis and the feeding ratio of precursor presented in Table 1 complies with broadness in OH stretching frequency by increasing dextran content in PGSD. On the other hand, linearity of PCL fraction with molecular weight (Table 1) with almost similar polydispersity index revealed the homogeneity of the PGD and confirms the formation of uni-model graft copolymer.

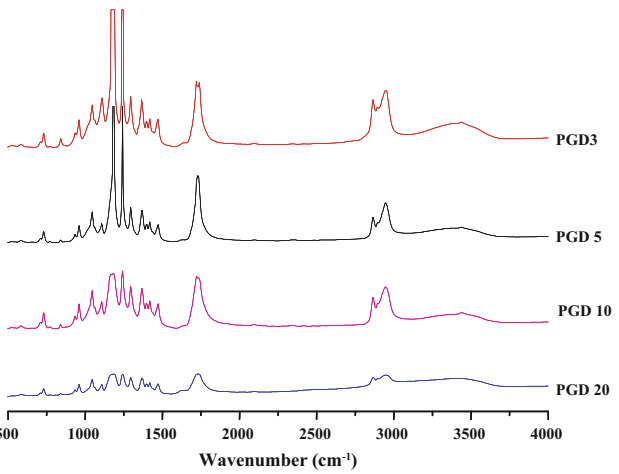

Fig. 1 FT-IR spectra of PGD copolymers (a) PGD-3 (b) PGD-5 (c) PGD-10 (d) PGD-20

Table 1 Different feed ratio and molecular weight of copolymers

Sample	Feed ratio (CL/OH of SD)	$(Sn(Oct)_2)$ (Met/OH of SD)	Fraction of PCL[a]	Mn[b]	Mw[b]	Poly disperse index
PGSD 20	20	0.05	0.94	21,600	31,800	1.47
PGSD 10	10	0.05	0.73	11,800	16,800	1.42
PGSD 5	5	0.02	0.18	8,950	12,900	1.44
PGSD 3	3	0.02	0.09	4,970	6,750	1.32

[a] Calculated by H-NMR

[b] Calculated by gel permeation chromatography (GPC)

3.2 Characterization of PGD NPs

3.2.1 Particle size and size distribution

Higher surface area to volume ratio of NPs provides more area for the encapsulated drug. The drug release from the NPs via diffusion and surface erosion and also have added advantage to penetrate and permeate through the physiological barriers. It was reported in the literature that smaller NPs would have greater ease of entry and durability in the tumors [23]. It was suggested that large particles (<5 μm) would be taken up via the lymphatics and small particles (<500 nm) can across the membrane of epithelial cells through endocytosis [24, 25]. Table 2 shows that particle size ranges from 141 nm to 191 nm with variation in polydispersity. Various factors such as solution property, thermodynamics, and preparation methods are responsible to control polydispersity index. In our case, as the particles were prepared in distilled water with neutral pH, the variation in polydispersity index of the nanoparticles may be due to the variation in polymer molecular weight.

3.2.2 Surface charge

Zeta-potential is one of the most important physicochemical characteristics of nanoparticles [26]. In the present study, we found that Zeta-potential was negative correlated with NPs (Table 2). High absolute value of zeta-potential indicates high electric charge on the surface of the NPs, which can cause strong repellent forces among particles to prevent aggregation of the NPs [27]. The NPs were found be negatively charged with a potential value ranging from −12.8 mV to −28 mV. An increase in the negative surface charge of the PGD NPs due to an increase in their size is observed.

3.2.3 Surface morphology

The surface and bulk morphology are also important in determining the drug release kinetics from the nanoparticles. The structure of the nanoparticles plays an important role in determining their adhesion to and interaction with cells. Surface analysis gives clear evidence for the effects of the coating material and emulsifiers on the nanoparticle surface, structure and the findings provide guidance in nanoparticle preparation [28]. The surface characteristics of the formulated PGD NPs were studied by AFM and presented in Fig. 2. The images showed that these nanoparticles have smooth surface morphology and narrow distribution in all the cases. Further, they appeared to be spherical and well dispersed with 130–150 nm average diameters.

3.3 In-vitro fluorescent marker release

The use of fluorescent markers in NPs visualization can lead to misinterpretation of NPs uptake data due to the leaching or dissociation of fluorescent markers into the released medium and hence subsequently into the cells [29]. Neither, could fluorometric analysis differentiate between intracellular and surface located particles, nor determine whether fluorescence detected was due to the cell-associated particles or the fluorescence released from the particles in the medium which was subsequently taken up by the cells. Thus, in vitro release study of fluorescence from the NPs specimen was conducted to confirm the results obtained mainly due to the cell-associated NPs but not from the released fluorescence in the medium. Figure 3 shows the in vitro release profiles of fluorescence markers from standard fluorescent PGD NPs. Data presented in this figure correspond to the average value of triplicates. We

Table 2 Characterization of PGD NPs copolymer nanoparticles

Property of samples	PGD-3	PGD-5	PGD-10	PGD-20
Particle size (nm)	141 ± 12	158 ± 15	164 ± 20	191 ± 8
Polydispersity	1.77 ± 0.02	1.34 ± 0.01	1.54 ± 0.02	1.93 ± 0.02
Zetapotential (mV)	−12.83 ± 3.2	−14.99 ± 4.0	−16.73 ± 6.5	−28.80 ± 2.1

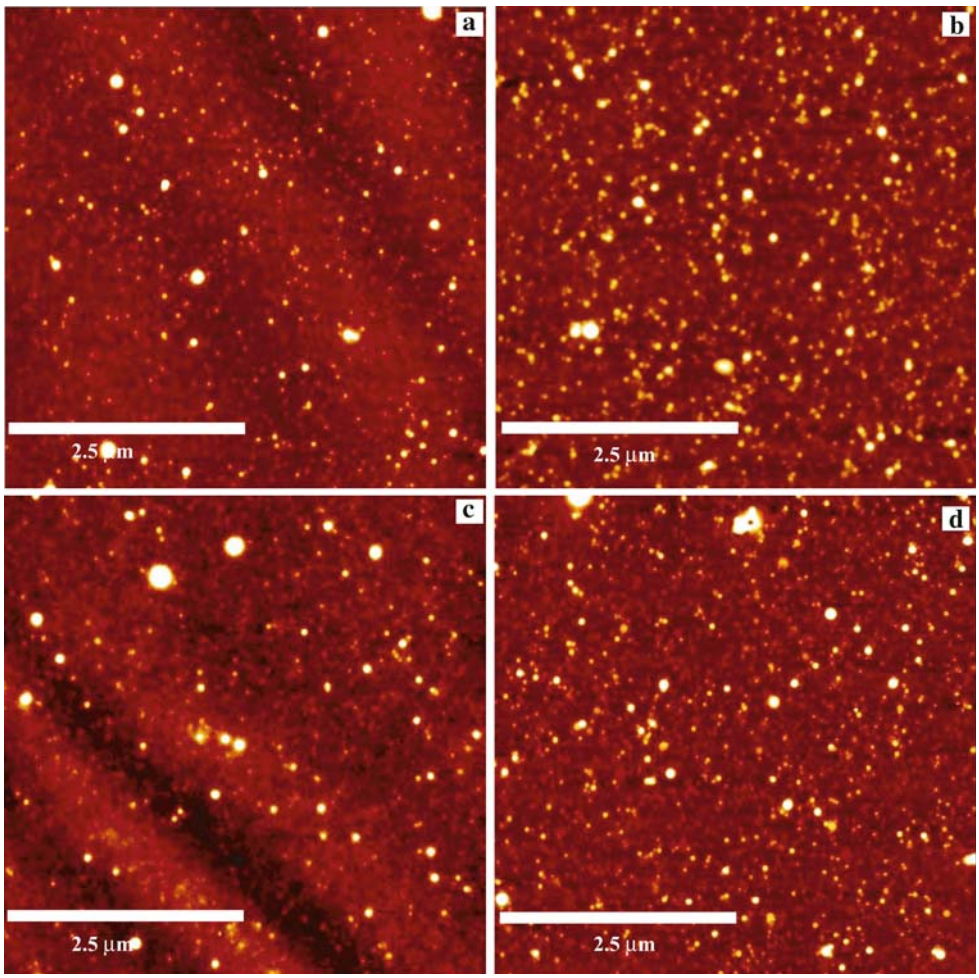

Fig. 2 AFM images of PGD NPs- (**a**) PGD-3 (**b**) PGD-5 (**c**) PGD-10 (**d**) PGD-20

found that the smaller the particle size, the faster release from the PGD NPs. This is quite understandable since the smaller the particle size, the larger the surface area per unit mass or volume. It can also be found from figure that the coumarin-6 was released around 15% from NPs, over 24 h incubation time, where as 4–8.5% of fluorescent release

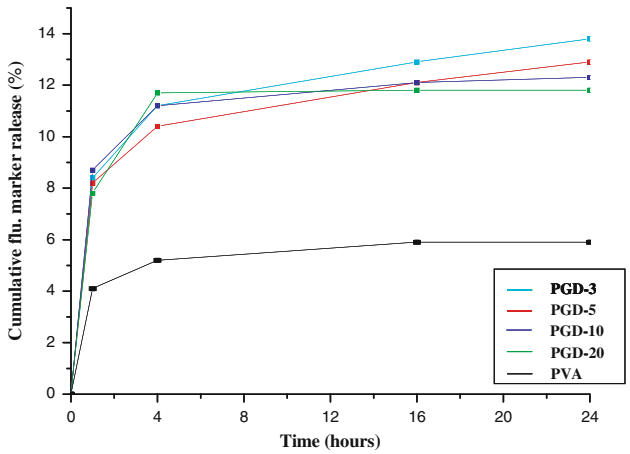

Fig. 3 In-vitro fluorescence marker release from PGD Nanoparticles

was found in 1 h and a sustained release was found after 4, 16, and 24 h in all the cases. The control experiments carried out using PVA did not show any significant uptake in comparison with the NPs uptake of the SNU 638 cells. It is thus reasonable to assume that most of the coumarin-6 was associated in the NPs and the fluorescence measured from the uptake samples mainly reflects the cellular associated fluorescent NPs but not the released fluorescence in the medium.

3.4 In-vitro cellular uptake of NPs

In the study of cellular uptake of NPs in in vitro or in vivo, the use of fluorescently or radioactively labeled NPs is the most common experimental approach found in the literature. Fluorescent labeling was chosen in the present study to avoid exposure of the samples to radioactive materials. Fluorescent labeling makes cellular uptake of NPs readily detectable by fluorescence microscopy or CLSM. The extent of particle uptake can then be determined by flow cytometry, fluorometry, or quantitative extraction of the

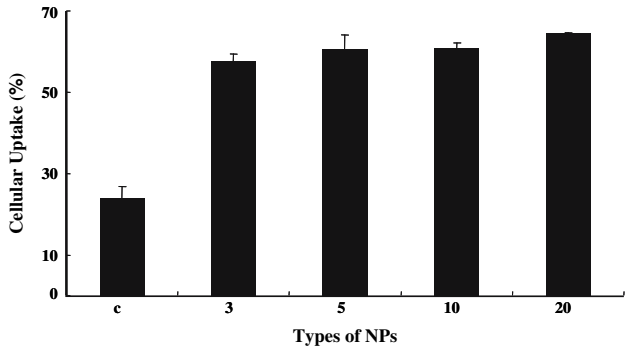

Fig. 4 Cellular uptake efficiency of SNU-638 with PGD NPs

markers from the cells [30, 31]. Cell line experiments are preferred as an initial study to provide preliminary information that helps to predict NPs are good for drug release. Cell line experiments give better reproducibility and allow screening of a higher number of samples compared to in vivo models [32]. In our study, SNU-638 cell line was used to investigate the cellular uptake of NPs.

Figure 4 demonstrates the quantitative cellular uptake efficiency of PGD NPs after 2 h incubation with SNU-638 cells with 50 μL of NPs, from the figure, it is clear that these PGD NPs showed 56–64% cellular uptake by the cells. In terms of the cellular uptake of different samples, PGD-3 showed two fold higher cellular uptake as compared to control (PVA), whereas both PGD-5 and PGD-10 had three fold greater uptake as compared to control groups. The NPs PGD-20 showed little more cellular uptake than that of PGD-5 and PGD-10. These results indicate that these biodegrdable PGD NPs have significant cellular uptake by SNU-638 cells, thus support the assumption that the NPs surface in contact with biological fluids, cells, or cellular components can be modified to provide favorite interactions with the cells [33]. The observed results also indicate that the NPs of 100–200 nm size can be used for cellular uptake experiments.

Confocal microscopic examination was carried out to assess the qualitative uptake of PGD NPs and presented in Fig. 5. From the images obtained, we understand that the fluorescence of the coumarin 6-loaded NPs (green) is closely located around the nuclei (stained red by propidium iodide), which indicates that the NPs have been taken up by the cells. It should be noted that the cell membrane has too small dimension (∼10 nm) to be recognized in this figure, in which the cells have dimension of ∼10 μm = 10,000 nm. It can thus be concluded that the fluorescent NPs are located inside the cells but not within the cell membrane. Therefore we report that the NPs showed quantitative and qualitative uptake by SNU-638 cells and thus can be useful in drug release application in sustained manner.

3.4.1 In-vitro cell viability

In order to understand the effect of the prepared PGD NPs on cell viability, they were treated with SNU-638 cells in the concentration of 50 μL of the PGD NPs per 3 mL of cell culture media. As shown in the Fig. 6, no cell death was noticed and the observed cell morphology also

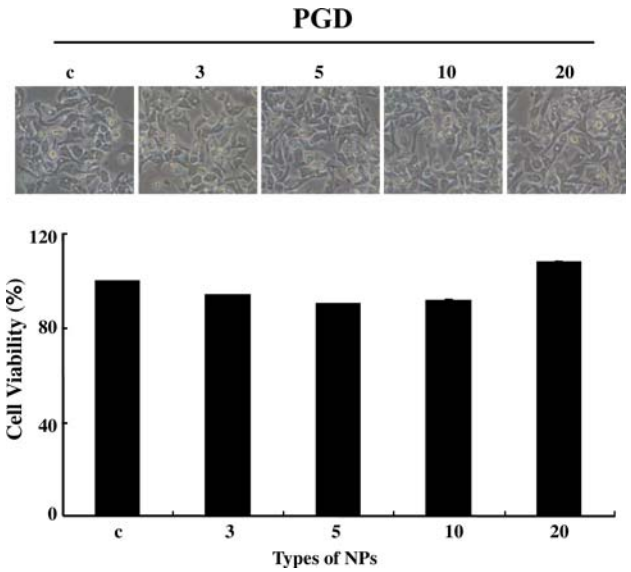

Fig. 6 In-vitro cell viability test of PGD Nanoparticles after 48 h

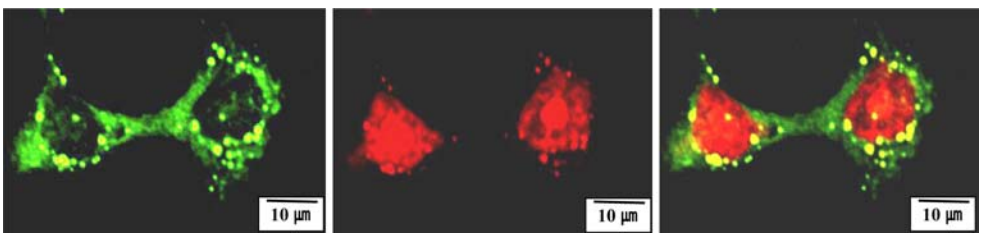

Fig. 5 Confocal microscopic images of SNU-638 cells after 2 h incubation with coumarin 6-loaded PGD-20 nanoparticles at 37 °C. The cells were stained by propidium iodide (red) and the uptake of fluorescence coumarin 6-loaded nanoparticles (green) in SNU-638 cells was visualized by overlaying images obtained by FITC filter and PI filter (right—image from combined PI channel and FITC channel; middle—image from PI channel; left—image from FITC channel)

revealed that there was no effect on the cell survival after treatment with the NPs for 48 h. Results of the cell viability test revealed that these NPs can be used as drug carrier without causing any damage to the cell on its own account.

4 Conclusion

In this study, biodegradable PGD graft copolymers synthesized by ring opening polymerization were utilized in the NPs formulation to check its drug carrying efficiency. The PGD NPs prepared by a oil/water emulsion method were found to have particle size ranging from 141 nm to 191 nm. The quantitative and qualitative cellular uptake of these NPs was carried out by treating with SNU-638 cells. In vitro Cell line experiments proved that these PGD NPs have shown great promise in cellular uptake by SNU-638 cells. The increased PGD NPs uptake by cancer cells indicates the possibility of using it as an anticancer drug carrier system for sustained release. Cell viability assessed after 48 h showed that these novel PGD NPs are non-toxic. Though the results obtained in our work are encouraging, further in vivo studies using animal model is needed to support them.

Acknowledgement This work was supported by the Korean Research Foundation Grant founded by the Korean Government (MOEHRD) (The Center for Health Care Technology Development, Chonbuk National University, Jeonju 561-756 Republic of Korea) and Korean Government Project No: 10028211, through Ministry of Commerce, Industry and Energy Department.

References

1. Cancer nanotechnology; US Department of Health & Human Service, National Institute of Health and National Cancer Institute, 2004
2. S. S. FENG, *Expert Rev. Med. Dev.* **1** (2004) 115
3. K. PETRAK, *Drugs Pharm. Sci.* **61** (1993) 275
4. L. GTISLAIN, P. COUVREUR, V. EBAERTS, M. ROLAND and L. SPEISER, *Int. J. Pharm.* **15**, (1983) 335
5. C. G. Pitt, New York. Marcel Dekker (1990) 71
6. A. P. D. ELFICK, *Biomaterials* **23** (2002) 4467
7. M. P. DESAI, V. LABHASETWAR, E. WALTER and R. J. LEVY, *Pharm. Res.* **14** (997) 1568
8. C. FONSECA, S. SIMOES, C. FONSECA and J. SIMOES, *J. Cont. Rel.* **83** (2002) 273
9. Y. N. KONAN, R. GURNY and Y. N. KONAN, *Int. J. Pharm.* **233** (2002) 239
10. G. GREGORIADIS, in "Drug Carriers in Biology and Medicine" (Academic Press, London, 1979) p. 107
11. M. J. POZNANSKY and L. G. CLELAND, in "Drug Delivery Systems" (Oxford University Press, New York, 1980) p. 253
12. T. W. SERY and E. J. HEHRE, *J. Bacterio.* **71** (1956) 71
13. C. PASSIRANI, G. BARRATT, J. P. DEVUSSAGUET and D. LABARRE, *Life Sci.* **62** (1998) 785
14. N. JAULIN, M. APPEL, C. PASSIRANI, G. BARRATT and D. LABARRE, *J. Drug Target.* **8** (2000) 165
15. C. PASSIRANI, G. BARRATT, J. P. DEVISSAGUET and D. LABARRE, *Pharm. Res.* **15** (1998) 1046
16. C. CHAUVIERRE, D. LABARRE, P. COUVREUR and C. VAUTHIER, *Macromolecules* **36** (2003) 6018
17. C. LARSEN, E. HARBOSE, M. JOHANSEN and H. P. OLESEN, *Pharm. Res.* **5** (1989) 995
18. I. YDENS, D. RUTOT, I. YDENS, J. SIX and P. DUBOIS, *Macromolecules* **33** (2000) 6713
19. C. NOUEL, I. YDENS, P. DUBOIS and J. SIX, *Polymer* **43** (2002) 1735
20. N. BHATTARAI, R. BHATTARAI, M. S. KHIL, D. R. LEE and H. Y. KIM, *Eur. Polym. J.* **39** (2003) 1603
21. K. Y. WIN and S. S. FENG, *Biomaterials* **26** (2005) 2713
22. S. Y. PARK, T. R. BILLIAR and D. W. SEOL, *Biochem. Biophys. Res. Commun.* **291** (2002) 150
23. Y. C. DONG and S. S. FENG, *Biomaterials* **25** (2004) 2843
24. R. SAVIC, L. B. LUO, A. EISENBERG and D. MAYSINGER, *Science* **300** (2003) 615
25. M. E. LEFEVRE, J. W. VANDERHOFF, J. A. LAISSUE and D. D. JOEL, *Experimential* **34** (1978) 120
26. G. GAUCHER, M. H. DUFRESNE, V. P. SANT, N. KANG, D. MAYSINGER and C. LEROUX, *J. Cont. Rel.* **109** (2005) 169
27. L. MU and S. S. FENG, *J. Cont. Rel.* **80** (2002) 129
28. S. S. FENG and G. F. HUANG, *J. Cont. Rel.* **71** (2001) 53
29. H. SUH, B. JEONG, F. LIU and S. W. KIM, *Pharm. Res.* **15** (1998) 1495
30. P. ARTURSSON, *Ther. Drug Carrier Syst.* **8** (1991) 305
31. S. YEE, *Pharm. Res.* **14** (1997) 763
32. M. BUTLER, in "Animal Cell Culture and Technology" (Oxford, IRL Press, 1996) p. 112
33. W. ZAUNER, N. A. FARROW and A. M. R. HAINES, *J Cont. Rel.* **71** (2001) 39